Animal Microbiome

RESEARCH

Open Access

Lawsonia intracellularis infection induces changes in microbial community function and composition associated with reduced pig growth and feed efficiency

Emma T. Helm[1,3], Eric R. Burrough[2], Nicholas K. Gabler[3] and Fernando L. Leite[4*]

Abstract

Background *Lawsonia intracellularis* and its resulting disease remains a troubling pathogen for pork producers worldwide. In the current experiment, we aimed to characterize the microbiome of pigs challenged with *L. intracellularis* through peak disease impact to better understand microbial community function and how microbial changes may contribute to disease and resulting decreased growth. Twenty-four *L. intracellularis* negative barrows were assigned to either *L. intracellularis* negative (NC) or *L. intracellularis* challenged (PC) treatment groups ($n = 12$ pigs/treatment). On days post-inoculation (dpi) 0, PC pigs were inoculated with *L. intracellularis*. Feed disappearance was monitored daily, body weights and fecal samples were collected weekly. At dpi 21, pigs were euthanized for sample collection and macroscopic lesion scoring.

Results Pigs challenged with *L. intracellularis* had sustained reductions in growth performance and feed intake throughout the 21-day period ($P < 0.001$). This was accompanied by changes to fecal microbial communities, particularly increased abundance of *Chlamydia suis* in challenged pigs at dpi 7, 14, and 21. Changes to microbial communities were also accompanied by differences in microbial metabolism, marked most notably by signatures of lesser amino acid biosynthesis and greater nucleotide synthesis in challenged pigs.

Conclusions In summary, *L. intracellularis* challenge produced reductions in growth and feed intake. This was accompanied by sustained changes to fecal microbial communities, particularly sustained increased abundance of *C. suis* in challenged pigs. Changes to microbial communities were also accompanied by differences in microbial metabolism which likely play a role disease.

*Correspondence:
Fernando L. Leite
fernando.leite@boehringer-ingelheim.com
[1]School of Animal Sciences, Virginia Tech, Blacksburg, VA 24061, USA
[2]Department of Veterinary Diagnostic and Production Animal Medicine, Iowa State University, Ames, IA 50011, USA
[3]Department of Animal Science, Iowa State University, Ames, IA 50011, USA
[4]Boehringer Ingelheim Animal Health USA Inc., Duluth, GA 30096, USA

Background

Lawsonia intracellularis, the causative agent of porcine proliferative enteropathy, is a microaerophilic intracellular bacterium that is problematic for pork producers worldwide. In growing pigs, *L. intracellularis* causes diarrhea, reduced growth performance, and reduced feed efficiency, significantly attenuating profitability [1, 2]. Disease is characterized by hyperproliferation of epithelial cells primarily in the terminal ileum, although disease may extend into the jejunum and colon [2, 3]. These changes lead to nutrient malabsorption, inflammation, intestinal dysbiosis, and reduced productivity [1–3]. One factor that likely influences *L. intracellularis* disease progression and pathogenesis is the intestinal microbiome. Previous research has demonstrated modulations to small intestinal, large intestinal, and fecal microbiomes resulting from *L. intracellularis* challenge [4–6], identifying several taxa that may serve as pathobionts during *L. intracellularis* challenge. However, research has only utilized 16 S rRNA sequencing, while shotgun metagenomic sequencing may permit for more specificity when determining changes to individual microbial species. Furthermore, the functional capacity of the intestinal microbiome during *L. intracellularis* challenge remains largely uncharacterized.

Therefore, the objective of this experiment was to characterize the fecal microbiome at various stages of *L. intracellularis* infection using shotgun metagenomic sequencing. Further, we aimed to characterize the functional changes to the microbiome and determine their association with production performance (growth, feed efficiency, feed intake) throughout disease progression. We also sought to better understand how bacteria other than *L. intracellularis* may be contributing to intestinal lesions by investigating bacterial localization through in situ hybridization in formalin-fixed tissues.

Materials and methods

All animal procedures were approved by the Iowa State University Institutional Animal Care and Use Committee (IACUC protocol #19–170) and adhered to the ethical and humane use of animals for research.

Animals, housing, and experimental design

This project was conducted as a subset of a study previously described [1]. In brief, 51 weaned barrows vaccinated for Porcine circovirus type 2 and *Mycoplasma hyopneumoniae* were randomly selected from a nonvaccinated herd with no known history of *L. intracellularis* (Midwest Research Swine, Gibbon, MN) and confirmed negative for *L. intracellularis* via individual fecal PCR and blood ELISA. These pigs were weaned at approximately 21 days of age and housed in a clean, isolated facility for the six-week nursery phase. Seven weeks after weaning, 24 pigs of average body weight (33 ± 2.3 kg BW) were selected and transported to Ames, IA. These 24 pigs were allocated to individual pens across 2 rooms in the same barn and assigned to individual treatment groups as follows (n = 12 pigs/treatment): 1) *L. intracellularis* negative (**NC**); and 2) *L intracellularis* challenged (**PC**). Pigs were *ad libitum* fed the same diet throughout the experiment which contained no antimicrobials, met or exceeded all NRC [7] requirements for this size pig, and has been published previously [1].

On days post inoculation (**dpi**) 0 (1 week after transport), the PC pigs were inoculated with *L. intracellularis* via gastric gavage (40 mL gavage containing 2.7×10^8 organisms/mL; determined by quantitative PCR). The inoculum was a crude intestinal homogenate collected from lesioned *L. intracellularis* positive pigs obtained through a commercial supplier (Gut Bugs Inc., Fergus Falls, MN, USA). The inoculum was tested previously by the supplier to be negative for the presence of different pathogens such as *Salmonella enterica*, porcine respiratory and reproductive syndrome virus, enterotoxigenic E*scherichia coli*, coccidian oocysts, and nematode eggs. Individual pig body weights were recorded on dpi 0, 7, 14, and 19. Individual pig feed disappearance was recorded between 0600 and 0800 h each day. From these recordings, individual pig average daily gain (**ADG**), average daily feed intake (**ADFI**), and feed efficiency (Gain: Feed; **G: F**) were calculated.

Fecal samples were collected from all pigs at dpi 0, 7, 14, and at necropsy. One sample was submitted to the Iowa State Veterinary Diagnostic Lab (**ISU VDL**) for quantitative PCR to evaluate *L. intracellularis* fecal shedding. A second fecal sample was frozen at -80° C until DNA extraction and microbiota analysis. On dpi 0, 7, 14, and necropsy, 10 mL blood samples were collected into BD Serum Vacutainer tubes (Becton, Dickinson and Company, Franklin Lakes, NJ) via jugular venipuncture from all pigs. Samples were centrifuged (2,000 x g for 10 min at 4° C), and serum was collected, aliquoted, and stored at -80° C until analysis. One aliquot was submitted to the ISU VDL prior to freezing to quantify *L. intracellularis* antibody response via the SVANOIR Ileitis ELISA (Indical Bioscience, Leipzig, Germany).

All pigs were euthanized at approximately dpi 21 (dpi 19–23). Pigs were euthanized in reps of 6–8 pigs per rep, with at least 2 NC pigs included in each necropsy rep. Necropsies were performed over several days to allow for completion of fresh tissue assays that have been previously published [1]. Pigs were euthanized by captive bolt followed by exsanguination for pathologic evaluation to confirm the challenge model. The methods for macroscopic and microscopic pathological scoring have been described in detail and results presented elsewhere [1].

DNA extraction, library preparation, and sequencing

Snap frozen fecal samples from dpi 0, 7, 14, and necropsy were stored at -80° C until DNA extraction and microbiota analysis at a commercial sequencing and bioinformatics facility (Cosmos ID, Germantown, MD). Fecal sample DNA was isolated using the QIAGEN DNeasy PowerSoil Pro Kit, according to the manufacturer's protocol. Extracted DNA samples were quantified using Qubit 4 fluorometer and Qubit™ dsDNA HS Assay Kit (Thermo Fisher Scientific, Waltham, MA).

DNA libraries were prepared using the Nextera XT DNA Library Preparation Kit (Illumina, San Diego, CA) and IDT Unique Dual Indexes with total DNA input of 1ng. Genomic DNA was fragmented using a proportional amount of Illumina Nextera XT fragmentation enzyme. Unique dual indexes were added to each sample followed by 12 cycles of PCR to construct libraries. DNA libraries were purified using AMpure magnetic Beads (Beckman Coulter, Brea, CA) and eluted in QIAGEN elution buffer (Germantown, MD). DNA libraries were quantified using Qubit 4 fluorometer and Qubit™ dsDNA HS Assay Kit. Libraries were then sequenced on an Illumina NextSeq 2000 platform 2 × 150 bp.

Microbiota bioinformatics

The CosmosID system (Germantown, MD) utilizes a high-performance data-mining k-mer algorithm that rapidly disambiguates millions of short sequence reads into the discrete genomes engendering the particular sequences [8]. The pipeline has two separable comparators: the first consists of a pre-computation phase for reference databases and the second is a per-sample computation. The input to the pre-computation phase are databases of reference genomes that are continuously curated by CosmosID scientists. The output of the pre-computational phase is a phylogeny tree of microbes, together with sets of variable length k-mer fingerprints (biomarkers) uniquely associated with distinct branches and leaves of the tree. The second per-sample computational phase searches the hundreds of millions of short sequence reads, or alternatively contigs from draft de novo assemblies, against the fingerprint sets. This query enables the sensitive yet highly precise detection and taxonomic classification of microbial NGS reads. The resulting statistics are analyzed to return the fine-grain taxonomic and relative abundance estimates for microbial NGS datasets. To exclude false positive identifications, the results are filtered using a filtering threshold derived based on internal statistical scores that are determined by analyzing a large number of diverse metagenomes.

Initial QC, adapter trimming and preprocessing of metagenomic sequencing reads are done using BBduk [9]. The quality-controlled reads are then subjected to a translated search against a comprehensive and non-redundant protein sequence database, UniRef 90. The UniRef90 database, provided by UniProt [10], represents a clustering of all non-redundant protein sequences in UniProt, such that each sequence in a cluster aligns with 90% identity and 80% coverage of the longest sequence in the cluster. The mapping of metagenomic reads to gene sequences are weighted by mapping quality, coverage and gene sequence length to estimate community wide weighted gene family abundances as described by Franzosa et al. [11]. Gene families are then annotated to MetaCyc [12] reactions (Metabolic Enzymes) to reconstruct and quantify MetaCyc [12] metabolic pathways in the community as described by Franzosa et al. [11]. Furthermore, the UniRef_90 gene families are also regrouped to GO terms [13] in order to get an overview of GO functions in the community. Lastly, to facilitate comparisons across multiple samples with different sequencing depths, the abundance values are normalized using Total-sum scaling (TSS) normalization to produce "Copies per million" (analogous to TPMs in RNA-Seq) units.

Chromogenic in-situ hybridization and image analysis

To further investigate associations between *L. intracellularis* and other bacteria at necropsy, previously fixed sections of the distal ileum [1] were trimmed, embedded in paraffin, sectioned at 4 µm, and mounted on SuperFrost® Plus glass slides (VWR™, Radnor, PA, USA) at the ISU VDL. Visualization and colocalization of RNA transcripts was performed using the RNAscope® 2.5 VS Duplex Kit (Advanced Cell Diagnostics, Newark, CA) with the procedure as instructed by the manufacturer and utilizing the Roche Ventana Medical Systems DISCOVERY ULTRA (Ventana Medical Systems, Inc., Tucson, AZ) as previously described [14] and employing probes B-L. intracellularis-aspA (cat. #464969) and EB-16 S-rRNA-C2 (cat. #464469-C2) with brown chromogen in channel 1 and red chromogen in channel 2. To visualize *Chlamydia*, a singleplex assay was run using the VS Universal AP kit with red chromogen and probe Ctr-16SrRNA (cat. #462749).

Quantification of *L. intracellularis* and eubacterial in situ hybridization (ISH) labeling within the ileum was performed using the HALO® image analysis platform (Indica Labs®, v3.4.2986, Albuquerque, NM). All slide preparations were converted to whole slide images using an Aperio® GT 450 slide scanner (Leica Biosystems®, Deer Park, IL). Regions of interest were manually annotated in each section of ileal tissue to include the mucosa while excluding the other intestinal layers and the lumen. ISH labeling was quantified as a percentage of labeled surface area for each probe/chromogen over the total surface area of the annotated region using the Area Quantification algorithm (v2.3.1).

Semi-quantitative assessment of *Chlamydia* labeling was performed using the following scale: 0 = no labeling detected, 1 = < 25% of villi have labeled bacteria, 2 = 25–50% of villi have labeled bacteria, and 3 = > 50% of villi have labeled bacteria.

Statistical analysis and data visualization

Statistical analysis of growth rates and feed intake, and serum assays were performed in SAS 9.4 (SAS Institute, Cary, NC). The following mixed model was fitted to quantitative parameters:

$$Y_{ijk} = \mu + \mathrm{Trt}_i + \mathrm{dpi}_k + (\mathrm{Trt} \times \mathrm{dpi})_{ij} + e_{ijk}$$

wherein Y_{ijk} = the phenotype measured on animal *k*; μ = the overall mean; Trt_i = effect of treatment (fixed effect; NC, PC); dpi_j = effect of time (fixed effect; dpi 0–7, 8–14, 15–21, or daily); (Trt x dpi)$_{ij}$ = interaction effect between treatment *i* and dpi *j*; e_{ijk} = error term of animal *k* subjected to treatment *i* in period *j*, $e_{ijk} \sim N(0, \sigma_e^2)$. When applicable, baseline measures were included as covariates in the model above. Least square (**LS**) means were determined using the LS means statement and differences in LS means were produced using the pdiff option. All data are presented as LS means with a pooled standard error of the mean (**SEM**).

Alpha diversity boxplots were calculated from abundance score matrices from CosmosID taxonomic analysis. Shannon alpha diversity metrics were calculated in R using the R package vegan [15]. Wilcoxon Rank-Sum tests were performed between groups using the R package ggsignif. Boxplots with overlaid significance in p-value format were generated using the R package ggplot2 [16],

Beta Diversity Principal Coordinate Analyses were calculated from relative abundance matrices from CosmosID taxonomic analysis. Bray-Curtis diversities were calculated in R using the R package Vegan with the functions vegdist, and PCoA tables were generated using Vegan's function pcoa [15]. PERMANOVA tests for each distance matrix were generated using Vegan's function adonis2. Plots were visualized using the R package ggpubr [17].

Linear Discriminant Analysis Effect Size figures were generated using the LEfSe tool from the Huttenhower lab, based on absolute abundance matrices from CosmosID taxonomic analysis [18]. LEfSe is calculated with a Kruskal-Wallis alpha value of 0.05, a Wilcoxon alpha value of 0.05, and a logarithmic LDA score threshold of 2.0.

Organism and metadata associations amongst *L. intracellularis* challenged pigs were generated using the MaAsLin2 tool from the Huttenhower lab, based matrices from CosmosID analysis [19]. For these analyses, a false discovery rate (*Q*-value) cutoff of 0.10 was utilized to determine significant correlations.

RNAscope ISH assay results were analyzed in JMP Pro version 16 (SAS Institute, Cary, NC). The Halo image analysis results for the duplex assay (*Lawsonia* and 16 S probes) were compared using a two-sided t-test to determine differences between treatments and a multivariate analysis to determine the correlation between labeling for the two probes. The semi-quantitative results from the *Chlamydia* singleplex assay were compared using Fisher's exact test. Results were considered significant if $P \leq 0.05$.

Results

Microbial composition of challenge material

Shallow shotgun sequencing of gut homogenate challenge material was performed to identify taxa present in the crude inoculum. Sequencing revealed the presence of 38 bacterial taxa. *Lawsonia intracellularis* was the most abundant taxa, at 18% of total reads. Other taxa present in lesser quantities included *Alistipes* sp. AM16-43, *Alistipes onderdonkii*, *Faecalibacterium prausnitzii*, and *Bacteroides stercoris* (Supplementary Table 1).

Response to challenge

Clinical ileitis is characterized by loose, formless stools, depression, and inappetence. In PC pigs, clinical ileitis was first observed on dpi 7 and pigs continued to show signs of disease throughout the experiment. In total, 100% of PC pigs showed signs of enteric disease; however, antimicrobial intervention was not required at any point during the experimental period. Pigs in the negative control group did not show clinical signs of enteric disease, their negative status was confirmed by serum antibody titers and fecal shedding of pathogen, which has been published in detail elsewhere [1]. Briefly, for antibody titers, pigs in the NC group remained negative while antibody titers in PC pigs increased from dpi 7–21. Similarly, fecal shedding of organism increased throughout the experiment for PC pigs, while NC pigs remained negative [1].

There was no difference in body weight gain, feed intake, or feed efficiency between treatment groups during the pre-challenge period (dpi −7 to 0, data not shown). In the post-challenge period, the treatment by dpi interaction was significant for change in body weight ($P < 0.001$, Fig. 1A). Body weight gain was linear throughout the study for NC pigs, and reductions in body weight change were observed in PC pigs compared with NC pigs. By dpi 21 (necropsy), NC pigs had gained 10 kg body weight more than their PC counterparts.

Similar to weekly body weight change, daily feed intake differed due to time ($P < 0.001$, Fig. 1B), treatment ($P < 0.001$), and the interaction of treatment and time was also significant ($P < 0.001$). In general, PC pigs had

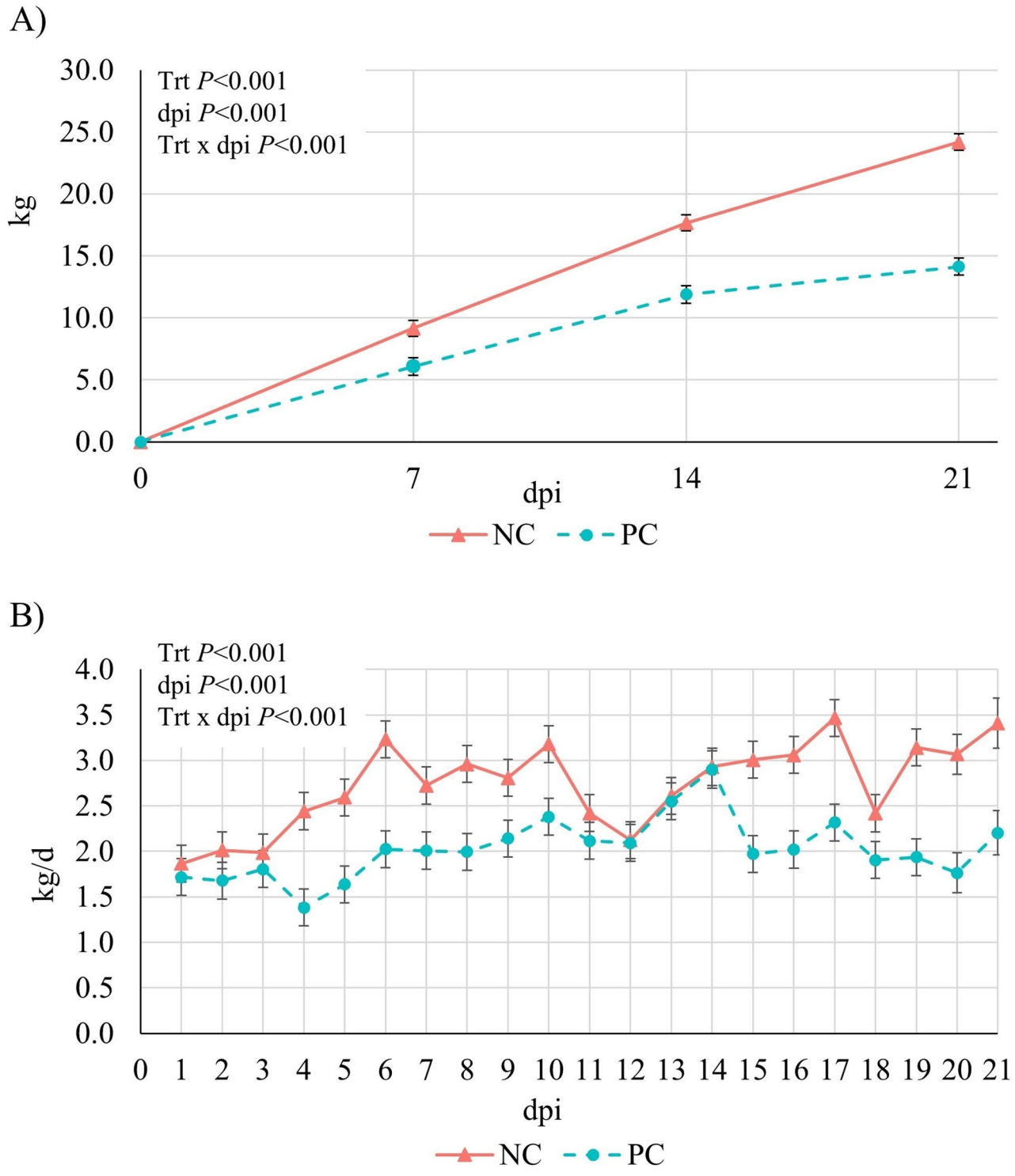

Fig. 1 Growth performance. A) change in body weights and B) daily feed intake in non-infected pigs (NC) and *Lawsonia intracellularis* inoculated pigs (PC) at different days post-inoculation (dpi). PC pigs were inoculated at dpi 0 and data were collected for 3 weeks. Data represents 12 pigs/treatment

reduced feed intake compared with NC pigs throughout the experiment. Reductions in feed intake were first observed around dpi 4 and continued to be reduced until dpi 12. From dpi 12–14, PC pigs appeared to have slight feed intake recovery, however their feed intake dropped around dpi 15 and remained lesser than that of PC pigs for the remainder of the experiment.

Fecal microbiome

Microbial composition was impacted by *L. intracellularis* challenge, relative abundance data is available in supplemental material 2. As expected, *L. intracellularis* abundance was significantly greater in fecal samples from PC pigs at dpi 14 and dpi 21. *Lawsonia intracellularis* was not detected by shallow shotgun sequencing in any samples from NC pigs, further confirming their negative status. There were no differences in alpha diversity (Shannon and Chao) observed at dpi 0, 7, 14, or 21 (Supplementary Fig. 1). Beta diversity, as assessed by Bray-Curtis dissimilarity, did not differ among treatments at dpi 0 (Fig. 2A, $P = 0.592$). However, community variation was present after infection, with beta diversity differing at dpi 7 ($P = 0.003$, $R^2 = 0.102$, Fig. 2B), 14 ($P = 0.003$, $R^2 = 0.115$, Fig 2C), and 21 ($P = 0.001$, $R^2 = 0.160$, Fig 2D).

At dpi 7, there were several differentially abundant bacterial species as determined by LEfSe analysis (Fig. 3B). Compared to the NC pigs, *Streptococcus alactolyticus*, *Bifidobacterium porcinum*, *Prevotella hominis*, *Mitsuokella multacida*, *Mitsuokella jalaludinii*, *Ligilactobacillus ruminis*, *Acidaminococcus intestini*, *Gemmiger formicilis*, and an unspecified *Olsenella* species were enriched in NC pigs, while *Dialister succinatiphilus*, *Streptococcus suis*, an unspecified *Akkermansia*, *Chlamydia suis*, *Escherichia coli*, *Desulfovibrio piger*, an unspecified *Ruminococcus*, an unspecified *Oscillibacter*, an unspecified *Ruminococcaceae*, *Lactobacillus johnsonii*, *Limosilactobacillus reuteri*, *Butyricicoccus*

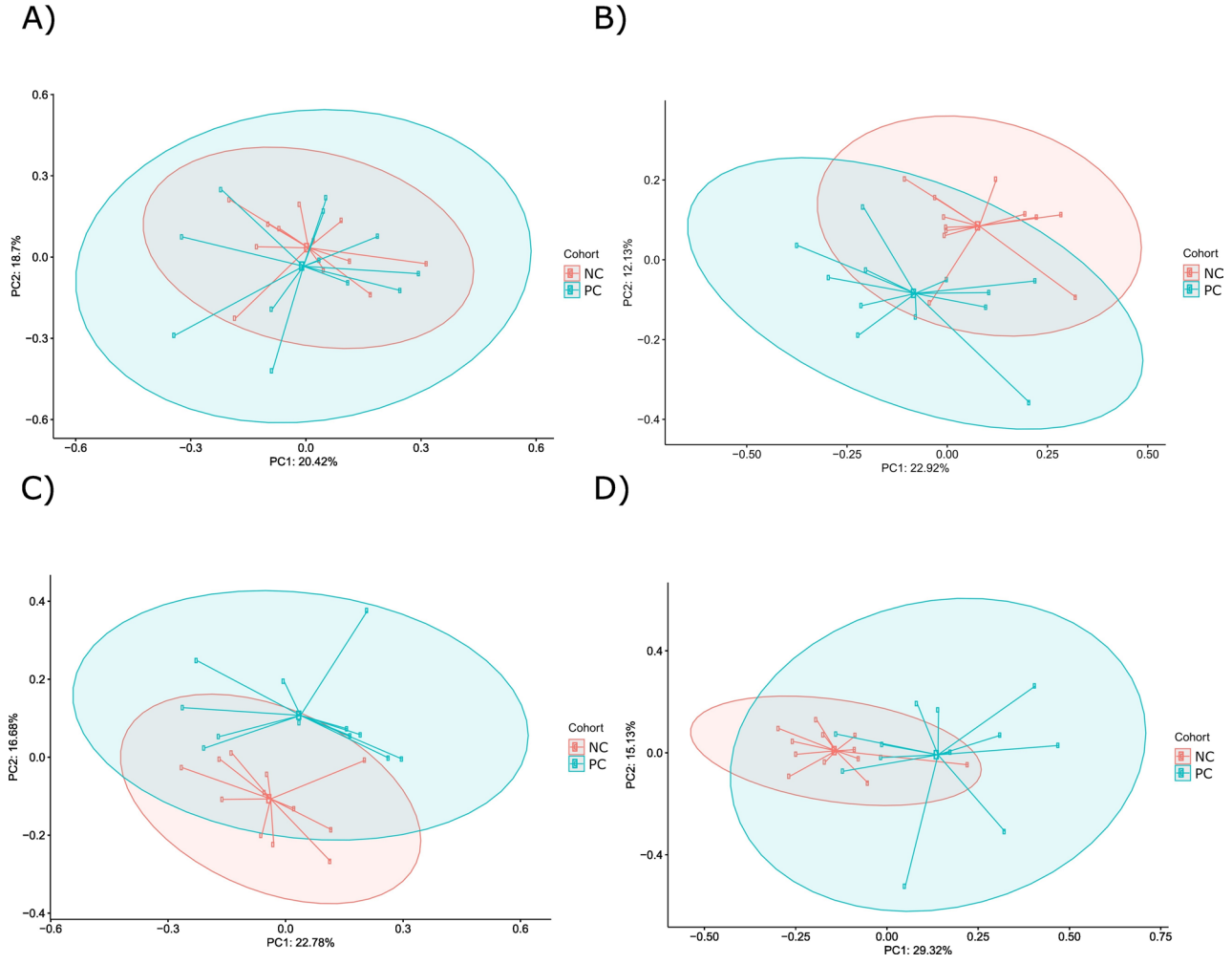

Fig. 2 Beta diversity (Bray-Curtis dissimilarity) of fecal microbiome in non-infected pigs (NC) and *Lawsonia intracellularis* inoculated pigs (PC) at days post inoculation (dpi) A) 0, B) 7, C) 14, and D) 21

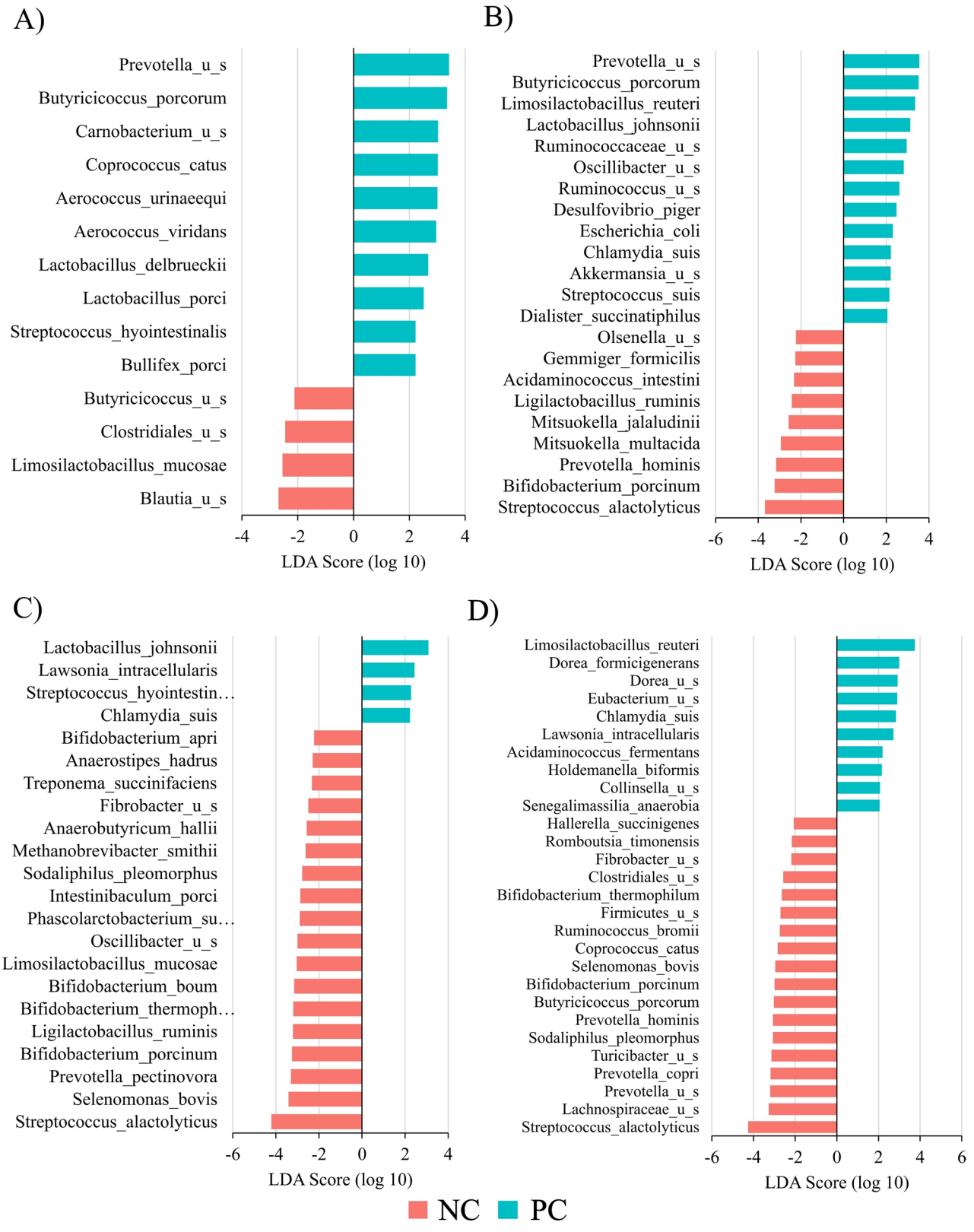

Fig. 3 Annotated results from linear discriminant analysis of differentially abundant microbial species at dpi A) 0, B) 7, C) 14, and D) 21 in feces of non-infected pigs (NC) and *Lawsonia intracellularis* inoculated pigs (PC). The histogram reveals differentially abundant taxa including increased abundance of *Chlamydia suis* in challenged pigs at dpi 7, 14, and 21

porcorum, and an unspecified *Prevotella* species were enriched in the PC pigs.

At dpi 14, *Streptococcus alactolyticus*, *Selenomonas bovis*, *Prevotella pectinovora*, *Bifidobacterium porcinum*, *Ligilactobacillus ruminis*, *Bifidobacterium thermophilum*, *Bifidobacterium boum*, *Limosilactobacillus mucosae*, an unspecified *Oscillibacter*, *Phascolarctobacterium succinatutens*, *Intestinibaculum porci*, *Sodaliphilus pleomorphus*, *Methanobrevibacter smithii*, *Anaerobutyricum hallii*, an unspecified *Fibrobacter*, *Treponema succinifaciens*, *Anaerostipes hadrus*, and *Bifidobacterium apri* were enriched in NC pigs. Conversely, *Chlamydia suis*, *Streptococcus hyointestinalis*, *L. intracellularis*, and *Lactobacillus johnsonii* were enriched in PC verses the NC pigs (Fig. 3C).

At dpi 21, *Streptococcus alactolyticus*, and unspecified *Lachnospiraceae*, and unspecified *Prevotella*, *Prevotella copri*, an unspecified *Turicibacter*, *Sodaliphilus pleomorphus*, *Prevotella hominis*, *Butyricicoccus porcorum*, *Bifidobacterium porcinum*, *Selenomonas bovis*, *Coprococcus catus*, *Ruminococcus bromii*, an unspecified *Firmicutes*, *Bifidobacterium thermophilum*, an unspecified *Clostridiales*, an unspecified *Fibrobacter*, *Romboutsia timonensis*, and *Hallerella succinigenes* were enriched in NC pigs while *Senegalimassilia anaerobia*, an unspecified *Collinsella*, *Holdemanella biformis*, *Acidaminococcus fermentans*, *Lawsonia intracellularis*, *Chlamydia suis*, an unspecified *Eubacterium*, an unspecified *Dorea*, *Dorea formicigenerans*, and *Limosilactobacillus reuteri* were enriched in PC pigs (Fig. 3D).

Chlamydia suis was the only bacterial species that was differentially abundant in PC pigs at three timepoints (dpi 7, 14, and 21), and was therefore selected for further analysis in fixed ileal tissues by in situ hybridization.

Microbiome metabolism (MetaCyc) and gene ontology

To establish if *L. intracellularis* challenge was associated with differences in metabolism of microbial populations, MetaCyc Pathway analysis was employed. At dpi 7, numerous pathways differed among groups (Fig. 4B).

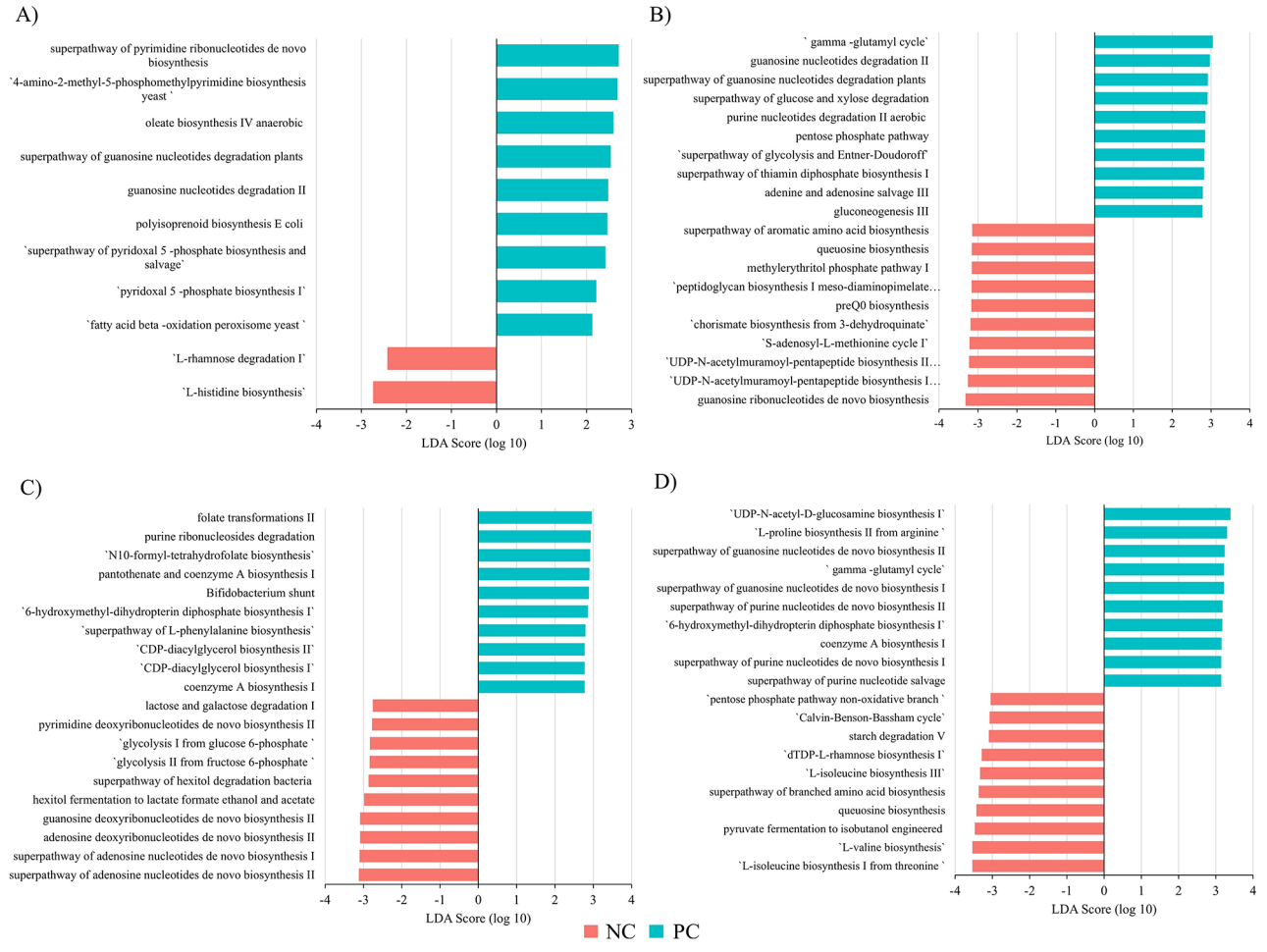

Fig. 4 Annotated results from linear discriminant analysis of differential MetaCyc pathways at days post inoculation (dpi) A) 0, B) 7, C) 14, and D) 21 in feces of non-infected pigs (NC) and *Lawsonia intracellularis* inoculated pigs (PC). The 10 most differentially enriched pathways in NC and PC groups are represented

Of these, pathways enriched in the PC pigs included gamma-glutamyl cycle (LDA = 3.04) and several pathways involving nucleotide degradation. The most enriched in NC pigs involved nucleotide (deoxyribo- and ribo-) biosynthesis, particularly guanosine. Additionally, several amino acid biosynthesis pathways were similarly enriched (or decreased due to infection in PC group).

At dpi 14, the MetaCyc pathway most enriched in PC pigs was the pathway for folate transformations (folate transformations II; LDA = 2.96; Fig. 4C). Several nucleotide/nucleoside degradation pathways were also enriched in PC pigs. Biosynthesis of several B vitamins and B vitamin derivatives (pantothenate, thiamin, N10-formyl-tetrahydrofolate, flavin) was also enriched in PC pigs at dpi 14. In the NC pigs enriched pathways included nucleotide biosynthesis, particularly superpathway of adenosine nucleotides de novo biosynthesis II (LDA = -3.11), superpathway of adenosine nucleotides de novo biosynthesis I (LDA = -3.09), and adenosine deoxyribonucleotides de novo biosynthesis II (LDA = -3.08). Several other nucleotides, including guanosine and pyrimidine, also had enriched de novo synthesis. Two amino acid synthesis superpathways and 2 glycolytic pathways were also enriched in NC pigs.

At dpi 21, 38 metabolic pathways were significantly enriched in PC pigs compared with NC pigs. This included UDP-N-acetyl-D-glucosamine biosynthesis I, a peptidoglycan precursor (LDA = 3.39), and 3 other peptidoglycan synthesis related pathways (Fig. 4D). Additionally, 12 nucleotide pathways were enriched in PC pigs, including pyrimidine deoxyribonucleotides biosynthesis from CTP, pyrimidine deoxyribonucleotides de novo biosynthesis III, pyrimidine deoxyribonucleotides de novo biosynthesis IV, superpathway of pyrimidine deoxyribonucleotides de novo biosynthesis *E coli*, pyrimidine deoxyribonucleotides de novo biosynthesis I, pyrimidine deoxyribonucleotide phosphorylation, superpathway of pyrimidine nucleobases salvage, superpathway of purine nucleotide salvage, superpathway of purine nucleotides de novo biosynthesis I, superpathway of purine nucleotides de novo biosynthesis II, superpathway of guanosine nucleotides de novo biosynthesis I, and superpathway of guanosine nucleotides de novo biosynthesis II.

In NC pigs, 23 bacterial metabolic pathways were enriched at dpi 21. These included several pathways related to amino acid synthesis (L-isoleucine biosynthesis I from threonine, L-valine biosynthesis, superpathway of branched amino acid biosynthesis, L-isoleucine biosynthesis III, L-histidine biosynthesis) and 4 glycolytic pathways (Fig. 4D).

Linear discriminant analysis was also employed to assess change in microbial gene ontology pathways in pigs challenged with *L. intracellularis* (Supplementary Fig. 2). These results were similar to that of changes to MetaCyc pathways, with no biological changes at dpi 0 and the greatest biological differences observed at dpi 21 (Supplementary Fig. 2C). At this time, 31 pathways were enriched in PC pigs compared with NC pigs, while 32 gene ontology pathways were enriched in NC pigs compared with PC pigs. We observed pathways such as DNA integration, zinc ion binding, and regulation of cell shape to be enriched in PC pigs, while several amino acid synthesis pathways (isoleucine biosynthesis, valine biosynthesis, histidine biosynthesis, leucine biosynthesis) were enriched in NC pigs.

Relationship between microbiome and production metrics

To investigate the association between production metrics and microbiome profiles (taxonomy and function) in PC pigs, we utilized Microbiome Multivariable Associations with Linear Models (MaAsLin 2) analysis. With this method, different microbial species, metabolic profiles, and gene ontology pathways were correlated to differences in other linear variables.

For species-level taxonomy, no bacterial taxa significantly correlated to production performance at any timepoint (ADG, ADFI, G:F). Furthermore, *L. intracellularis* did not correlate with any other variables such as fecal shedding or lesion length, despite being detected in PC pigs by metagenomic sequencing.

MetaCyc pathway analysis was used to investigate if bacterial metabolic pathways related to differences in production performance. There were no significant correlations among PC pigs at dpi 0, dpi 7 or dpi 14 (Supplementary Table 2). At dpi 21, 2 pathways positively correlated with ADG at dpi 21 (putrescine biosynthesis IV and thiazole biosynthesis I E. coli). We also observed thiazole biosynthesis I *E. coli* to be negatively correlated with G: F at dpi 21. Conversely, 4 pathways demonstrated a positive correlation with G: F and primarily included those related to sugar (galactose, sucrose, stachyose) degradation.

We also examined correlations with microbial gene ontology pathways over the course of infection. There were no significant correlations at dpi 0, 7, or 14, however there 76 pathways that demonstrated significant correlations ($Q < 0.100$) at dpi 21 (Supplementary Table 3). The strongest negative correlations were those associated with G: F, and included pathways such as bacterial type flagellum hook, homoserine O-acetyltransferase activity, and tRNA methylation. The strongest positive correlations were those associated with ADG and included X2-succinyl-5-enolpyruvyl-6-hydroxy-3-cyclohexene-1-carboxylic-acid synthase activity, phosphorelay response regulator activity, isochorismate synthase activity, and motile cilium.

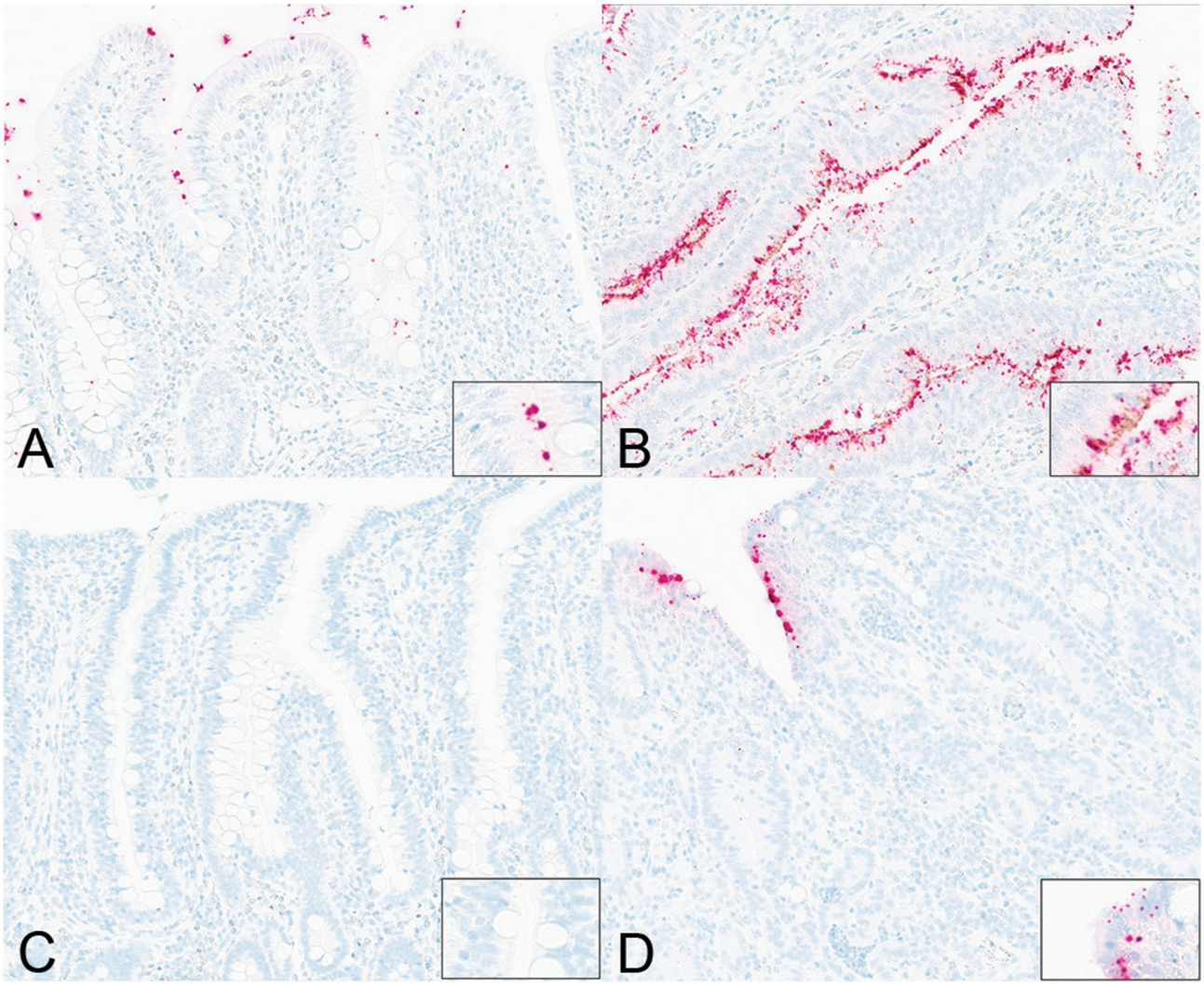

Fig. 5 Panels A and B are representative images from RNAscope ISH assessment of the *L. intracellularis* aspA gene (brown signal) and a16S rRNA eubacterial probe (red signal) in the ileum of NC (**A**) and PC (**B**) pigs at dpi 21. *L. intracellularis* was only detected in PC pigs and often colocalized with the eubacterial probe. Insets are higher magnification showing specific probe labeling in the cytoplasm and along the surface of enterocytes. Panels C and D are representative images from ISH assessment of *Chlamydia* in the ileum of NC (**C**) and PC (**D**) pigs at dpi 21. Insets are higher magnification of villus enterocytes. Labeling was only noted in PC pigs and most commonly within enterocytes at the luminal aspects of villi

Visualizing the relationship between *L. intracellularis* and other bacterial taxa

To further assess the relationship between *L. intracellularis* and other bacterial taxa at the site of infection, microscopic evaluation of ileal sections was performed at dpi 21. This included colocalization of *L. intracellularis* and other bacteria, as well as the specific localization of *Chlamydia*.

As expected, there was a significant ($P = 0.0103$) increase in *L. intracellularis* positive labeling in the PC pigs compared with NC pigs (Fig. 5A and B). Similarly, there was greater tagging of the 16 S eubacterial probe in the ileum of PC pigs compared with NC pigs ($P = 0.0136$). These two targets were often colocalized within the apical cytoplasm of enterocytes and within the lamina propria and there was a significant correlation between the percent positive area for each probe in the PC pigs ($r = 0.9826$, $P < 0.0001$). Most staining of both probes was in enterocytes rather than the lamina propria.

Chlamydia was only detected by ISH in PC pigs and was detected in 11 of 12 PC pigs ($P < 0.001$). A majority of PC pigs (9 of 12) had ISH scores of 1 while two had a score of 2 and no pigs had a score of 3. Interestingly, *Chlamydia* labelling was observed primarily on the luminal aspects of the villi, rather than within the hyperplastic crypts (Fig. 5D).

Discussion

Lawsonia intracellularis remains one of the most significant pathogens for pork producers worldwide [20, 21]. However, despite being highly prevalent and highly detrimental to productivity, much still remains unknown regarding its pathogenesis. In particular, the impact of *L. intracellularis* on the intestinal microbiome in the context of production performance and feed intake remains incompletely characterized. Thus, this study aimed to investigate the fecal microbiome of pigs at several stages of disease progression and relate microbiome profiles to production performance metrics.

Reductions in growth performance, feed intake, and feed efficiency have been well reported during *L. intracellularis* challenge [22–24], and was further confirmed herein. By the end of the 21-day challenge, NC pigs were nearly 10 kg heavier than their PC counterparts. Although we did not follow these pigs through disease resolution, it is unlikely PC pigs would have ever been able to fully recapitulate this body weight difference, resulting in additional days to market and reduced profitability. Additionally, although it is known *L. intracellularis* reduces feed intake, this is the first known report demonstrating daily changes to feed consumption. Our results indicate that reductions in feed intake can be observed as early as 4 dpi, and remain lessened throughout the 21-day period, despite observing day-to-day variation that can be expected with daily feed intakes. Interestingly, we did observe slight recovery of feed intake of PC pigs around dpi 12–14. Although the reasoning for this is unclear, it may be indicative of early immune responses attempting to clear the pathogen. Regardless, the sustained reductions to growth performance metrics observed herein provided an excellent model to investigate how the fecal microbiome is altered throughout a 21-day challenge period.

The pig's resident microbiota plays an important role in development of porcine proliferative enteropathy. Gnotobiotic pigs inoculated with a pure culture of *L. intracellularis* do not develop signs of disease, whereas those inoculated with a gut homogenate or several other bacterial taxa do show classic signs of disease [22, 25]. However, the exact bacterial taxa that may allow for disease development remain unknown. Previous research has implicated several genera, including *Chlamydia*, *Fusobacterium*, and *Bacteroides*, specifically *F. nucleatum* and *B. fragilis* [4]. In the current experiment, we also observed *Chamydia*, specifically *Chlamydia suis*, to be enriched in PC pigs at dpi 7, 14, and 21. *Chlamydia suis* is known to cause intestinal dysbiosis and enteritis in pigs [26, 27]. Interestingly, we did not detect this taxa in the challenge material as Leite et al. [4] did and this bacteria was only present in 5/24 pigs at dpi 0, perhaps the dysbiosis associated with *L. intracellularis* challenge allowed for its colonization and opportunistic expansion. To further assess the abundance and localization of *C. suis*, we used RNAscope to visualize *C. suis* transcripts in PC and NC pigs at dpi 21. As expected, *C. suis* abundance was greater in PC pigs; however, it appeared to remain localized to the luminal surface of the ileum, rather than being found in the hyperplastic crypts. Thus, while *C. suis* may not directly interact with intestinal crypts to influence the heightened proliferative state of intestinal epithelial cells, its interaction with *L. intracellularis* during disease progression warrants further investigation. We also observed several other pathogenic taxa to be enriched in the PC group, including *E. coli* and *S. suis* at dpi 7 and *S. hyointestinalis* at dpi 14, suggesting dysbiosis caused by *L. intracellularis* allows for the opportunistic expansion of other pathogens. This is further supported by the increase in bacteria labeled by the eubacterial 16 S probe in the PC pigs at dpi 21 and the strong correlation of this labeling with the presence of *L. intracellularis* in the apical cytoplasm of enterocytes in this study. Interestingly, 16 S staining of eubacteria did not reveal a major signal in the lamina propria as could be expected with a loss of intestinal integrity, this is aligned with previous data that transepithelial resistance isn't altered by *L. intracellularis*, despite the pathology caused [1].

Previous researchers have implicated *Prevotella* spp. to play a role in *L. intracellularis* disease progression. Vaccination against *L. intracellularis* decreased *Collinsella* and altered the abundance of *Prevotella* spp. in *L. intracellularis* and *Salmonella enterica* co-infected pigs [5], with some taxa decreasing in abundance while others increased. Furthermore, *Prevotella* decreased in vaccinated pigs compared with non-vaccinated pigs when challenged with *L. intracellularis* [4]. In the current study, while an unspecified genus of *Prevotella* was increased in PC pigs at dpi 7, *Prevotella* spp. were not observed to be significantly enriched by *L. intracellularis* challenge at dpi 21. In fact, several genera of *Prevotella* were enriched in NC pigs, including *P. pectinovora* at dpi 14 and *P. hominis*, *P. copri*, and an unspecified *Prevotella* at dpi 21. This finding is consistent with those of Hankel et al. [6], who observed *Prevotella* (closely matching *P. copri*) to be enhanced in non-clinical pigs compared with clinically afflicted pigs during field challenge. While the meaning of these discrepancies is not fully understood, a number of factors may have led to these observations. Firstly, previous studies of microbiome during *L. intracellularis* challenge have employed 16 S rRNA sequencing rather than shotgun metagenomics [4, 5], which differ in accuracy and consistency [28]. Further, the current study provides results at the species, rather than genus, level. The *Prevotella* genus is wide and diverse, while some may serve as pathobionts, others may be part of a beneficial and healthy microbiota [29]. Regardless, it did not appear

as though any *Prevotella* spp. served as pathobionts during *L. intracellularis* challenge in the current experiment.

Additionally, we aimed to evaluate some of the functional aspects of the microbiota that may change in response to *L. intracellularis* challenge. It is difficult to discern whether these shifts are more likely host-driven (altered nutrient availability due to disease) or microbe-driven (expansion of specific taxa). Prior to peak infection (dpi 7 and 14) fewer microbial pathways were differentially enriched, however of those several nucleotide degradation pathways were enriched in PC pigs at both timepoints. It is possible that these changes are due to nutrient scarcity, requiring microbes to utilize alternate energy sources. Feed intake reductions in PC pigs were observed as early as dpi 4, however immature epithelial cell proliferation, and therefore malabsorption, does not typically begin until dpi 11–14 [3, 30]. Thus, it is possible that there is a period of time where intestinal microbes have lower nutrient availability until disease progression impairs nutrient utilization in the pig.

As expected, we observed the most differences in functional aspects of the microbiota at dpi 21. This revealed 2 distinct functional profiles: in NC pigs, we observed enrichment of several pathways related to amino acid biosynthesis, whereas several pathways related to nucleotide synthesis were enriched in PC pigs. Previous researchers have also observed relationships between microbial amino acid synthesis and efficiency of feed utilization. In pigs genetically selected for diverging feed efficiency, residual feed intakes, microbial amino acid metabolism and biosynthesis were positively correlated with feed efficiency [31, 32], suggesting that the microbiota of more feed efficient pigs synthesizes more amino acids. In the current study, given that NC pigs have better feed efficiency and nitrogen digestibility [1], dietary amino acids may be of a lesser abundance in the lumen of the healthy pigs, thus microbes need to synthesize amino acids for their own use. Conversely, in the PC pigs, dietary utilization of feedstuffs, including protein, is significantly impaired [1], thus the microbiota does not need to synthesize their own amino acids. Several ruminal bacterial species demonstrate *de novo* synthesis of amino acids, including *Streptococcus bovis*, *Selenomonas ruminantium*, and *Prevotella bryantii* [33, 34]. Although these specific taxa were not observed to be enriched in NC pigs, it is possible species such as *Streptococcus alactolyticus* and *Selenomonas bovis*, which were enriched, may play a role in this mechanism.

In the PC pigs, we observed consistent upregulation of pathways related to nucleotide metabolism at dpi 21, specifically pathways related to biosynthesis of purine nucleotides. Interestingly, there appears to be a critical link between nucleotide biosynthesis and pathogenesis of several bacterial taxa, including *Staphylococcus aureus*, *E. coli*, and *Salmonella* Typhimurium [35]. When purine synthesis pathways are mutated, intracellular pathogen *Salmonella* Typhimurium is more susceptible to death by reactive oxygen species [36] and growth of other intracellular pathogens is reduced when purine biosynthesis pathways are mutated [35]. In fact, when *E. coli* is mutated to have disruptions to purine and pyrimidine synthesis pathways, its ability to colonize mouse intestine is significantly diminished [37]. It is possible that *L. intracellularis* also utilizes purine biosynthesis as a mechanism to acquire nucleotides for replication and the increase in purine biosynthesis pathways reflects the increase of *L. intracellularis* in the pig's intestine. Bacteria are able to communicate through a variety of networks to act as a functional unit and regulate activities such as replication [38], so signaling crosstalk may result in the global upregulation of nucleotide synthesis pathways across the microbial community. Alternatively, increased microbial nucleotide synthesis is associated with resistance to radiation treatment in rectal cancer patients, suggesting microbiota-mediated nucleotide metabolism increased the nucleotide pool for hyperproliferation of rectal tumors, a similar pathology as to what is observed during *L. intracellularis* challenge [3, 39]. It is possible the signaling pathways responsible for cell proliferation in the pig have some crosstalk with the microbiota, leading to greater microbial nucleotide synthesis and replication. Thus, greater microbial replication would result in a greater demand for nucleotides, warranting their synthesis. It is also possible that these changes in metabolism are a response to changes in the intestinal niche; *L. intracellularis* is known to reduce the abundance of goblet cells and thus mucus production [2, 40], which would alter substrates available to the microbiome for metabolism and replication.

Despite increased knowledge of the pig microbiome and how microbial profiles may be altered by disease states such as *L. intracellularis*, there remains a dearth of information relating microbial profiles to production performance metrics in the context of disease. Thus, we leveraged Microbiome Multivariable Associations with Linear Models (MaAsLin) to determine if we could correlate specific microbial taxa, metabolic pathways, or both with reductions in performance amongst diseased pigs. However, we did not observe any bacterial taxa to be significantly correlated to production performance at any timepoint (ADG, ADFI, G:F). This was initially surprising, considering *L. intracellularis* was detected by sequencing and via microscopy in challenged pigs. However, sample size for correlation analyses in this study was significantly limited (12 PC pigs), perhaps in a larger group of diseased pigs these relationships would be better observed. Without observing the causative bacterial taxa to have any correlation with disease presentation,

it is challenging to interpret correlations to metabolic pathways and/or gene ontology pathways with much confidence, although changes to their abundance among challenge and control groups still shed important light on disease and were potentially found due to having a stronger correlation than that of the single *L. intracellularis* pathogen.

Conclusions

In summary, *L. intracellularis* challenge produced reductions in growth and feed intake. This was accompanied by sustained changes to fecal microbial communities, particularly sustained increased abundance of *C. suis* in challenged pigs, which may serve as a pathobiont during *L. intracellularis* challenge. Changes to microbial communities were also accompanied by differences in microbial metabolism, marked most notably by signatures of lesser amino acid biosynthesis and greater nucleotide synthesis in challenged pigs, likely playing a role in the development of disease and accompanying decrease in growth and feed efficiency.

Supplementary Information

The online version contains supplementary material available at https://doi.org/10.1186/s42523-025-00501-0.

Supplementary Material 1

Supplementary Material 2

Acknowledgements
The authors would like to thank Dr. Dana Beckler and the staff at Gut Bugs, Inc. for providing inoculum and housing pigs during the nursery phase of this project.

Author contributions
All authors contributed to study design and sample collection. EH, EB, and FLL performed laboratory analyses and data analyses. EH drafted the manuscript. All authors have contributed to data interpretation and manuscript revision. All authors have read and approved the final manuscript.

Funding
This study was funded by Boehringer Ingelheim Animal Health USA Inc. The study was designed by NG, EB, EH, and FLL and accepted by Boehringer Ingelheim Animal Health USA Inc. Boehringer Ingelheim Animal Health USA Inc. did not provide any sort of inference in data analysis, data interpretation or drafting of the manuscript, thus all information presented here is merely based on scientific data.

Data availability
The authors confirm that the data supporting the findings of this study are available within the article and its supplementary materials. Raw sequence data generated and/or analyzed during the current study are not publicly available due to restrictions imposed by the funding body but are available from the corresponding author on reasonable request.

Declarations

Ethics approval and consent to participate
All animal procedures were approved by the Iowa State University Institutional Animal Care and Use Committee (IACUC protocol #19–170) and adhered to the ethical and humane use of animals for research.

Consent for publication
All authors have read the manuscript and agreed on publication in its current version.

Competing interests
The authors declare that they have no competing interests. FL is employed by Boehringer Ingelheim Animal Health USA Inc., however there is no competing interest as no product was evaluated in this study.

Received: 14 August 2025 / Accepted: 24 November 2025
Published online: 05 January 2026

References

1. Helm ET, Burrough ER, Leite FL, Gabler NK. Lawsonia intracellularis infected enterocytes lack sucrase-isomaltase which contributes to reduced pig digestive capacity. Vet Res. 2021;52:90.
2. Vannucci FA, Guedes RMC, Gebhart CJ. Lawsonia. In *Diseases of Swine.* 12th edition. Edited by Zimmerman JJ, Burrough ER, Karriker LA, Schwartz KJ, Zhang J. West Sussex: Wiley-Blackwell; 2025:1009–1022.
3. Leite FL, Abrahante JE, Vasquez E, Vannucci F, Gebhart CJ, Winkelman N, Mueller A, Torrison J, Rambo Z, Isaacson RE. A cell proliferation and inflammatory signature is induced by lawsonia intracellularis infection in swine. MBio. 2019;10:e01605–01618.
4. Leite FL, Winfield B, Miller EA, Weber BP, Johnson TJ, Sylvia F, Vasquez E, Vannucci F, Beckler D, Isaacson RE. Oral vaccination reduces the effects of lawsonia intracellularis challenge on the swine small and large intestine Microbiome. Front Vet Sci. 2021;8:692521.
5. Leite FLL, Singer RS, Ward T, Gebhart CJ, Isaacson RE. Vaccination against lawsonia intracellularis decreases shedding of Salmonella enterica serovar typhimurium in Co-Infected pigs and alters the gut Microbiome. Sci Rep. 2018;8:2857.
6. Hankel J, Sander S, Muthukumarasamy U, Strowig T, Kamphues J, Jung K, Visscher C. Microbiota of vaccinated and non-vaccinated clinically inconspicuous and conspicuous piglets under natural Lawsonia intracellularis infection. Front Vet Sci. 2022;9.
7. National Research Council. Nutrient requirements of swine: eleventh revised edition. Washington, DC: National Academies; 2012.
8. CosmosID. CosmosID Metagenomics Cloud. app.cosmosid.com.
9. Bushnell B. BBDuk guide. DOE Joint Genome Institute. http://www.jgi.doe.gov/data-and-tools/software-tools/bbtools/bb-tools-user-guide/bbduk-guide. 2021.
10. UniProt Consortium T. UniProt: the universal protein knowledgebase. Nucleic Acids Res. 2018;46:2699–2699.
11. Franzosa EA, McIver LJ, Rahnavard G, Thompson LR, Schirmer M, Weingart G, Lipson KS, Knight R, Caporaso JG, Segata N. Species-level functional profiling of metagenomes and metatranscriptomes. Nat Methods. 2018;15:962–8.
12. Caspi R, Foerster H, Fulcher CA, Kaipa P, Krummenacker M, Latendresse M, Paley S, Rhee SY, Shearer AG, Tissier C. The metacyc database of metabolic pathways and enzymes and the biocyc collection of Pathway/Genome databases. Nucleic Acids Res. 2007;36:D623–31.
13. Clarke LL. A guide to Ussing chamber studies of mouse intestine. Am J Physiol Gastrointest Liver Physiol. 2009;296:G1151–1166.
14. Chen Y-M, Helm ET, Groeltz-Thrush JM, Gabler NK, Burrough ER. Epithelial-mesenchymal transition of absorptive enterocytes and depletion of peyer's patch M cells after PEDV infection. Virology. 2021;552:43–51.
15. Oksanen J, Blanchet FG, Kindt R, Legendre P, Minchin PR, O'hara R, Simpson GL, Solymos P, Stevens MHH, Wagner H. Package 'vegan'. Community Ecol Package Version. 2013;2:1–295.
16. Ahlmann-Eltze C, Patil I. ggsignif: Significance Brackets for 'ggplot2'. R package version 0.6.0.2019.
17. Kassambara A. ggpubr:'ggplot2'based publication ready plots. R package version 0.4.0.2020.
18. Segata N, Izard J, Waldron L, Gevers D, Miropolsky L, Garrett WS, Huttenhower C. Metagenomic biomarker discovery and explanation. Genome Biol. 2011;12:R60.
19. Mallick H, Rahnavard A, McIver LJ, Ma S, Zhang Y, Nguyen LH, Tickle TL, Weingart G, Ren B, Schwager EH. Multivariable association discovery in population-scale meta-omics studies. PLoS Comput Biol. 2021;17:e1009442.

20. Arnold M, Crienen A, Swam H, von Berg S, Jolie R, Nathues H. Prevalence of lawsonia intracellularis in pig herds in different European countries. Porcine Health Manage. 2019;5:1–11.
21. Marsteller TA. Monitoring the prevalence of lawsonia intracellularis IgG antibodies using serial sampling in growing and breeding swine herds. J Swine Health Prod. 2003;11:127–30.
22. McOrist S, Lawson GH. Reproduction of proliferative enteritis in gnotobiotic pigs. Res Vet Sci. 1989;46:27–33.
23. Paradis MA, Gebhart CJ, Toole D, Vessie G, Winkelman NL, Bauer SA, Wilson JB, McClure CA. Subclinical ileitis: diagnostic and performance parameters in a multi-dose mucosal homogenate challenge model. J Swine Health Prod. 2012;20:137–42.
24. Gogolewski RP, Cook RW, Batterham ES. Suboptimal growth associated with Porcine intestinal adenomatosis in pigs in nutritional studies. Aust Vet J. 1991;68:406–8.
25. McOrist S, Mackie R, Neef N, Aitken I, Lawson G. Synergism of ileal symbiont intracellularis and gut bacteria in the reproduction of Porcine proliferative enteropathy. Vet Rec. 1994;134:331–2.
26. Aumayer H, Leonard CA, Pesch T, Prähauser B, Wunderlin S, Guscetti F, Borel N. Chlamydia suis is associated with intestinal NF-κB activation in experimentally infected gnotobiotic piglets. Pathog Dis. 2020;78.
27. Schautteet K, Vanrompay D. Chlamydiaceae infections in pig. Vet Res. 2011;42:1–10.
28. Xu W, Chen T, Pei Y, Guo H, Li Z, Yang Y, Zhang F, Yu J, Li X, Yang Y, et al. Characterization of shallow Whole-Metagenome shotgun sequencing as a High-Accuracy and Low-Cost method by complicated mock microbiomes. Front Microbiol. 2021;12:678319.
29. Amat S, Lantz H, Munyaka PM, Willing BP. Prevotella in pigs: the positive and negative associations with production and health. Microorganisms. 2020;8:1584.
30. Guedes RMC, Machuca MA, Quiroga MA, Pereira CER, Resende TP, Gebhart CJ. Lawsonia intracellularis in pigs: progression of lesions and involvement of apoptosis. Vet Pathol. 2017;54:620–8.
31. Jiang H, Fang S, Yang H, Chen C. Identification of the relationship between the gut Microbiome and feed efficiency in a commercial pig cohort. J Anim Sci. 2021;99:skab045.
32. McCormack UM, Curião T, Buzoianu SG, Prieto ML, Ryan T, Varley P, Crispie F, Magowan E, Metzler-Zebeli BU, Berry D. Exploring a possible link between the intestinal microbiota and feed efficiency in pigs. Appl Environ Microbiol. 2017;83:e00380–00317.
33. Lin R, Liu W, Piao M, Zhu H. A review of the relationship between the gut microbiota and amino acid metabolism. Amino Acids. 2017;49:2083–90.
34. Atasoglu C, Valdés C, Walker ND, Newbold CJ, Wallace RJ. De Novo synthesis of amino acids by the ruminal bacteria prevotella Bryantii B14, selenomonas ruminantium HD4, and Streptococcus Bovis ES1. Appl Environ Microbiol. 1998;64:2836–43.
35. Goncheva MI, Chin D, Heinrichs DE. Nucleotide biosynthesis: the base of bacterial pathogenesis. Trends Microbiol. 2022;30:793–804.
36. Mantena RK, Wijburg OL, Vindurampulle C, Bennett-Wood VR, Walduck A, Drummond GR, Davies JK, Robins-Browne RM, Strugnell RA. Reactive oxygen species are the major antibacterials against Salmonella typhimurium purine auxotrophs in the phagosome of RAW 264.7 cells. Cell Microbiol. 2008;10:1058–73.
37. Vogel-Scheel J, Alpert C, Engst W, Loh G, Blaut M. Requirement of purine and pyrimidine synthesis for colonization of the mouse intestine by Escherichia coli. Appl Environ Microbiol. 2010;76:5181–7.
38. Ng WL, Bassler BL. Bacterial quorum-sensing network architectures. Annu Rev Genet. 2009;43:197–222.
39. Teng H, Wang Y, Sui X, Fan J, Li S, Lei X, Shi C, Sun W, Song M, Wang H. Gut microbiota-mediated nucleotide synthesis attenuates the response to neoadjuvant chemoradiotherapy in rectal cancer. Cancer Cell. 2023;41:124–38. e126.
40. Huan YW, Bengtsson RJ, MacIntyre N, Guthrie J, Finlayson H, Smith SH, Archibald AL, Ait-Ali T. Lawsonia intracellularis exploits beta-catenin/Wnt and Notch signalling pathways during infection of intestinal crypt to alter cell homeostasis and promote cell proliferation. PLoS ONE. 2017;12:e0173782.

Publisher's note